Nanomaterials-protein interactions: the case of pristine and functionalized carbon nanotubes and Porcine Gastric Mucin (PGM)

Nanomaterials-protein interactions: the case of pristine and functionalized carbon nanotubes and Porcine Gastric Mucin (PGM)

Nadia Barbero[a], Marco Marenchino[b], Ramón Campos-Olivas[b], Simonetta Oliaro-Bosso[c], Luca Bonandini[a], Jasminka Boskovic[b], Guido Viscardi[a] and Sonja Visentin[d]*

[a]Department of Chemistry and NIS Interdepartmental Centre, University of Torino, via Pietro Giuria 7, 10125 Torino, Italy

[b]Structural Biology and Biocomputing Programme, Spanish National Cancer Research Centre (CNIO), NMR Unit, Madrid, Spain

[c]Department of Drug Science and Technology, University of Torino via P. Giuria 9, 10125 Torino, Italy

[d]Molecular Biotechnology and Health Sciences Department, University of Torino, via Quarello 15, 10135 Torino, Italy.
sonja.visentin@unito.it

Abstract

Mucus represents a serious obstacle that prevents the penetration of drug ~~carriers~~ transport across the mucus barrier. This study highlights the interaction between mucin glycoprotein, mucin from porcine stomach Type III (PGM), and different pristine and functionalized single wall and multi wall carbon nanotubes (CNTs), under physiological conditions, in order to investigate the affinity of different CNTs to mucin. This aspect could be of the utmost importance for the use of CNTs for biomedical purposes. The interaction between CNTs and PGM was investigated by using different techniques like fluorescence steady-state spectroscopy, thermogravimetric analysis (TGA), dynamic light scattering (DLS), circular dichroism (CD), electrophoresis, scanning electron microscopy (SEM) and transmission electron microscopy (TEM). We demonstrated that mucin has impressive capabilities for binding CNTs in physiological solutions. Moreover, we proved that the interaction is influenced by the different nature of the tubes (SW and MW) and the different functionalization (pristine and oxidized CNTs).

Keywords

Single-wall Carbon Nanotubes, Multi-wall Carbon Nanotubes, Porcine Gastric Mucin, Interaction

Introduction

Epithelial layers in the body are protected from pathogens and similar stresses by mucus, a complex hydrophilic mixture whose function and regulation are involved in numerous diseases, such as cystic fibrosis, asthma, and cancer.(Hattrup and Gendler 2008) Mucus is composed primarily of water (95%), but it also contains salts, lipids, proteins with defensive purpose and growth factors.(Bansil and Turner 2006) The mucus barrier represents a serious obstacle that prevents the penetration of therapeutic xenobiotics across epithelial lining of the gut to the systemic circulation. Hence, drug and drug carriers transport across the mucus barrier is important to enhance drug bioavailability and the correlated biological effect. Although its importance from a medical and physiological point of view, the principles that regulate the permeability of mucus of drugs and nanomaterials remain unknown.

The main component that is responsible for mucus viscous and elastic gel-like properties is the glycoprotein mucin. The defensive mechanism of mucin is based on its lipo- and hydrophilic regions which form low affinity bonds with any particulates that come in contact with it. Two main mechanisms limit the diffusion through the gel: a) interaction with mucous components (i.e electrostatic and hydrophobic interactions); b) size filtering related to the size of the mesh spacing between mucin fibers. The first mechanism concerns both drugs in solution and nanoparticles while the second becomes relevant for nanoformulations.(Sigurdsson et al. 2013) In a mucin hydrogel the concentration of polymers defines the mesh size of the protein network. This mesh size sets the threshold beyond which the nanoparticles diffusion is inhibited: particles with dimension smaller than this mesh size should be able to pass through the hydrogel, whereas larger particles should not.(Lieleg et al. 2010) On the other hand in cervical mucus smaller particles can be immobilized more efficiently and the permeability of PEG functionalized polymeric nanoparticles will be enhanced in respect to non functionalized NPs. All these data suggest that the size filtering is not sufficient to clarify the mechanism of permeability and that some interactions with the protein has to be considered. Obviously these interactions are mediated by the nature of the nanomaterial and on particle surface properties.

The use of nanoparticles to deliver drugs across the mucus barrier may provide a significant advantage to current strategies. Among the available nanomaterials, carbon nanotubes (CNTs) have emerged as a new alternative and efficient tool for transporting and translocating therapeutic molecules.(Liu et al. 2009) CNTs offer a number of advantages for delivering drugs to specific locations inside the body suggesting that they may result more efficient than nanoparticles. CNTs have a large inner volume which allows more drug molecules to be encapsulated, and this volume is

more easily accessible because the end caps can be easily removed, and they have distinct inner and outer surfaces for functionalization.(Liu 2013) Recent research has shown the ability of CNTs to carry a variety of molecules such as drugs, DNA, proteins, peptides, targeting ligands etc. into cells, which makes them suitable candidates for targeted delivery applications.(He et al. 2013; Saifuddin et al. 2013)

Recently it was demonstrated that functionalized carboxyl nanoparticles (NPs) enhance mucus dispersion and hydration suggesting that, in chronic diseases involving mucus hypersecretion, obstruction and increased viscosity, negatively-charged functionalized polystyrene NPs may serve as effective mucus decongestants and dispersants.(Chen et al. 2010; Chen et al. 2012) Belgorodsky(Belgorodsky et al. 2010) showed that mucin Type I can bind and solubilize water-insoluble pristine CNTs in physiological solutions. Thus, CNTs can be oxidized, giving CNTs with hydrophilic groups such as OH and COOH.(Biale et al. 2009) Strong acid solution treatments can create defects in the side walls of CNTs, and the carboxylic acid groups are generated at the defect point, predominantly on the open ends. The resulting functionalized CNTs are more soluble in water and the carboxylic groups provide opportunities for further derivatization of the CNTs through esterification or amidation reactions.

Following these recent papers, we studied the interaction between mucin glycoprotein, mucin from porcine stomach Type III (PGM), and different pristine and functionalized single wall and multi wall CNTs, under physiological conditions, in order to investigate the affinity of different CNTs to mucin. After the complex formation, the different samples were characterized by UV-Vis, fluorescence spectroscopy, TGA, DLS, circular dichroism, electrophoresis, SEM and TEM.

Materials and methods

The carbon nanotube samples used were single (SWCNT) and multiwall (MWCNT) both pristine and oxidized form: pristine SWCNTs (p-SW), oxidized SWCNTs (o-SW), pristine MWCNTs (p-MW), oxidized MWCNTs (o-MW). Oxidation procedure is described in our previous papers (Mussi et al. 2010; Visentin et al. 2010) (see ESI for the procedure and the materials description). Mucin used was Type III, bound sialic acid 0.5-1.5 %, partially purified powder (Sigma, see ESI). CNTs (3 mg), both pristine and oxidized, were added to a solution of mucin protein (4 mg/mL) in 2 mM sodium phosphate buffer, pH 7.2 and the mixture was stirred for 12 h at room temperature. The reaction mixture was then filtered through a 0.45 μm filter and loaded on a Sephadex G-25 gel-permeation column. The protein complexes were eluted with a sodium phosphate buffer and the elution was monitored by UV/Vis and fluorescence spectroscopy. For a further characterization, the CNT-protein solutions were lyophilized and, when necessary, redissolved in water indicating the

absence of irreversible aggregation during the freeze-drying process. The UV/Visible spectra obtained closely resembled those reported for the MWCNT-Mucin dispersion by Belgorodsky et al.(Belgorodsky et al. 2010) (see Figure S1).

UV/Visible and Fluorescence spectroscopy.

UV-Visible measurements were recorded using a Shimadzu UV-1700 Pharma Spec Spectrophotometer equipped with 1.0 cm path length quartz cells. Fluorescence measurements were recorded using a LS55 Perkin Elmer spectrofluorimeter equipped with a xenon lampsource, a 5 mm path lenght quarz cell and a thermostat bath. Fluorescence spectra were recorded in the range of 290–450 nm upon excitation at 270 nm. Excitation and emission slits widths were 5/5 nm.

Thermogravimetric analysis.

TGA experiments were performed on approximately 10 mg of the samples under a 100 ml/min N_2 flow (heating ramp 10°C/min) by a TA instrument Q600 SDT Simultaneous DSC-TGA heat flow analyser. Percentage weight change versus temperature was evaluated over the range of 25–1000 °C.

Non denaturing Polyacrylamide Gel Electrophoresis (ND-PAGE).

The samples of Mucin, CNT and mucin-CNT complexes were prepared in gel loading buffer containing 10% glycerol and 0.01% bromophenol blue. Electrophoresis was performed using a 4% running gel without both SDS and 2-Mercaptoethanol. After electrophoresis the gel was stained for carbohydrate detection with periodic acid/Schiff (PAS) (Sigma).(Doerner and White 1990) As control, mucin (Sigma) and mucin processed in the same manner of complexes but without CNTs were used.

Circular Dichroism.

Circular dichroism (CD) measurements were performed on a Jasco-810 Dichrograph equipped with a Peltier thermoelectric controller. The spectra of the protein sample at 1 mg/mL were recorded in the continuous mode between 340 and 200 nm at 25°C. Thermal denaturation experiments were performed at constant heating rates of 60 °C/h by following the ellipticity at 208 nm from 5 to 95 °C in 0.1 cm path length quartz cuvette (Hellma) with a total protein concentration of 1 mg/mL in PBS buffer. The transition temperature (Tm) was estimated by direct non-linear least-squares fitting

of the temperature dependent ellipticity θ208 according to a two state model.(Scawen and Allen 1977)

Dynamic Light Scattering.

DLS data were collected using a DynaPro Instrument (DynaPro-99-E-50). DLS data were collected for 1 mg/mL for free mucin and 0.8 mg/mL for the samples of mucin/complexes. All hydrodynamic radii (RH) data reported were modelled as isotropic spheres and result from mass-weighted calculations. Polydispersity is defined as the relative standard deviation of RH measurements and expressed as % of polydispersity (%PD). The polydispersity of each peak is indicated by the width. Populations with polydispersity <15% are considered monodispersed, whereas those with values >15% are considered polydispersed. Data show that different CNTs will generate different aggregates with different polydispersity (Table 1).

Transmission Electron Microscopy.

Samples of mucin and purified mucin/CNTs complex were applied to glow-discharged carbon-coated copper grids, negatively stained with 2% uranyl acetate (w/v) and observed in Technai G2 Spirit transmission electron microscope at an accelerating voltage of 120 kV. Sample images were recorded at a nominal magnification of 21000 X.

Scanning Electron Microscopy.

SEM Samples of porcine gastric mucin and the purified complexes have been analysed by means of a Zeiss Evo50 scanning electron microscope with an accelerating voltage of 20kV and a magnification of 30000 and 40000 X.

Results and Discussion

The fluorescence spectra of mucin and of the mucin-CNTs samples are shown in Figure 1. Fluorescence spectra demonstrate the formation of protein/CNTs complexes for all the samples tested. Mucin alone shows a strong fluorescence emission at 360 nm and its fluorescence intensity is evident in the spectra of mucin-CNTs complexes while CNTs alone do not show any fluorescence.

The formation of CNT-protein complexes was further investigated by thermogravimetric analysis. TGA experiments were conducted in nitrogen and were performed on pristine nanotubes (p-SW and p-MW), oxidized CNTs (o-SW and o-MW) as well as on CNT-mucin complexes and mucin alone.

The complex formation follows a similar behaviour for both kinds of CNTs: the complex formation is greater for functionalized tubes rather than pristine CNTs. As shown in Figure 2 pristine CNTs were stable and showed a small weight loss starting at 600 °C (red line). Oxidized CNTs exhibited a non-negligible weight loss over the entire temperature range while mucin showed a strong degradation with a weight loss of 85%. The analysis of the first derivative of the thermograms shows that mucin has two main weight losses around 58 °C and 260°C. TGA of the complexes (mucin/CNTs) exhibited a weight loss of 70%, with a degradation around 280°C proving the formation of the complex (see Figures S2 and S3). The difference in the derivative temperature (mucin alone and CNT/mucin) upon heating is an indication that protein/CNT is not a mechanical mixture but it is adsorbed on the carbon nanotubes surface, as previously reported for similar systems.(Viterbo et al. 2004)

Once we established and proved the formation of the mucin/CNTs complex, we then exploited DLS and TEM in order to characterize and evaluate the overall sizes of the formed complexes. As quality control, we performed DLS measurement on a standard protein such as human serum albumin (HSA) (See Figure S4). Figure 3 (A-C) shows the light scattering intensity distribution of free mucin as well as in presence of different CNTs. TEM images (Figure 3) show that the protein seems to form irregular aggregates whose size is in agreement with the diameter of 305 nm retrieved by DLS analysis. As shown in panel B complexes formed between SW and mucin form irregular aggregate of different sizes, while complexes obtained by the reaction between MW and mucin (C) are completely different. In fact as shown by DLS and TEM analysis it seems that MWs tend to incorporate mucin on the length of the tubes while mucin englobes the SW tubes in a hank-like form.

Table S1 reports the Hydrodynamic Radius (R_H) and Polydispersity (PD) data for the species with major contribution. The results confirmed the data obtained by TEM analysis of the samples. The native mucin was present in three populations of particles with sizes near 25 nm, 300 nm, and > 3.5 μm as shown in panel A, in agreement with the R_H value of 305.7 nm found by DLS (see Table S1). The DLS analysis for the mucin/SW determined an increase in the size of the particles by up to 50% together with an increase in the PD factor (from 11.5% of mucin alone to 53.7% and 63.9% for mucin/p-SW and mucin/o-SW respectively), irrespective of the degree of oxidation of CNTs, probably corresponding to mucin coated by several CNTs. The presence of SW seems to cause the intertangling of fibrous structure through hydrophobic cross-linking, forming aggregates especially for o-SW. On the contrary, the DLS measurements of mucin with MWCNTs showed the disappearance of the particle near 25 nm and the presence of two populations near 200 nm and > 3.5

μm, the latest being the majority. These species are presumably free mucin and CNT of various lengths and bundles.

The particular behaviour of MW and SW has led us to further investigate and compare these two types of carbon nanotubes. SEM characterization reveals a nanostructured mat-type structure of mucin-MW or SW complex both for pristine and oxidized samples (Figure 4). Pristine samples do not show evidence of noticeable CNTs on the surface, but the presence of bright clusters and spots suggests CNTs emerging from the bulk. o-MW and o-SW samples reveal a complex structure with a more homogeneous arrangement of CNTs among mucin on the surface arranging in a lattice suggesting more affinity between mucin and oxidized CNTs.

Since SW CNTs are more interesting for biological purposes because of their lower toxicity compared to that of MW CNTs, we decided to investigate in detail the interaction SWCNT/mucin. To characterize the interaction of SW CNTs with PGM we performed a non denaturing electrophoresis using a 4% gel as the running gel (Figure 5). Literature data showed that CNTs in PAGE electrophoresis stopped at the interface of the 4% stacking gel and the loading wells.(Wang et al. 2009) After PAS staining, a sharp pink coloured band appeared at the bottom of the running gel in all lanes containing mucin (alone or in presence of CNTs). This faster running band was accompanied by 2 or 3 slower running bands faintly coloured (possibly higher molecular weight mucin aggregates) at the top of the gel. In lane 3 (mucin/o-SW complex) we observed at the top of the gel a single thick band (red arrow in Figure 5), possibly corresponding to a complex of mucin with oxidized CNTs. In correspondence of lane 2 (mucin/p-SW complex) a feeble band is present always at the top of the gel. These observations are consistent with the hypothesis of the formation of a complex between mucin and CNTs, mainly when SW are oxidized.

In order to investigate the possibility of CNTs bringing about any conformational changes in mucin, CD spectrum of the protein was analyzed in the presence of o-SW. Mucin macromolecule consists of four(Snary et al. 1970) or five(Carlstedt et al. 1985; MacAdam 1993) protein subunits (Mr 380-720 kDa(Marriott and Gregory 1990)) enriched in proline, glutamate, glycine, serine, threonine and valine(Carlstedt et al. 1985; MacAdam 1993)) and covalently bonded with carbohydrate side-chains. The spectra of free mucin in PBS and mucin/o-SW are shown in Figure 6a in the range between 250 and 200 nm that reflects the secondary structural features of proteins. The spectra are characterized by a single minimum near 205 nm. This λ min is significantly shifted from the λmin of a typical random coil (195 nm)(MacArthur and Thornton 1991) and it is characteristic of a polyproline rich helical structure(Ronish and Krimm 1974). Similar spectra were found for both samples suggesting that the presence of CNT did not alter the secondary structure content of mucin. A similar finding was observed in a previous study of adsorption of CNT to lysozyme(Bomboi et al.

2011). Spectra are nearly super-imposable, in particular at the wavelength of the minimum, suggesting that CNTs do not alter the secondary structure of mucin upon adsorption to the protein (Figure 6a). Furthermore we exploited thermal unfolding to investigate any stabilization of the protein induced by the presence of the o-SW. Figure 6b shows the thermal unfolding for free mucin and for the mucin/o-SW complex. Free mucin showed a transition temperature of 47 ºC in agreement to previous values obtained by fluorescence(Loomis et al. 1987). Since the protein has both hydrophobic and hydrophilic regions with the ability to form H-bonds and electrostatic interactions, from this experiment we can say that the presence of o-SW CNTs did not affect the transition temperature of mucin suggesting that the nature of the interaction is weak and restricted to the hydrophobic surface more than inside the hydrophobic cavities formed by the mucin protein (Figure 3b).

Conclusions

In this paper we investigated the binding of CNTs with the commercial available porcine gastric mucin. ~~We can say that~~ an interaction between CNTs and PGM occurs. This finding is evident from the quenching of the protein fluorescence by CNTs due to the formation of a protein-nanomaterial complex. These data show clearly that the microenvironment of mucin was changed during the binding interaction both with SW and MW CNTs. Other instrumental techniques such as TGA, SEM and TEM confirmed this interaction. We also demonstrated that the superficial functionalization of the material has a great influence on the binding.

Belgorodsky et al.(Belgorodsky et al. 2010) studied the interaction of bovine submaxillary mucin (BSM) glycoprotein with three different kinds of nanomaterials: fullerene-like WS_2, C_{60} fullerene and MWCNTs. In particular, they demonstrated that BSM showed impressive and unique capabilities in the binding and solubilizing of water-insoluble materials in physiological solutions.

In the present work, we have demonstrated that also porcine gastric mucin PGM has impressive capabilities for binding CNTs in physiological solutions. Moreover, we also made a comparison between SW- and MW-CNTs, both pristine and oxidized, showing the different behaviour which depends on the different nature of the tubes.

The understanding of the interaction between nanomaterials and mucins is of considerable current interest because of the many biomedical applications.

Acknowledgements

The authors thank University of Torino (Ricerca Locale ex-60%, Bando 2014). SV acknowledges financial support by NANOMED project (PRIN 2010-2011, 2010FPTBSH_003) from Ministero

dell'Istruzione, dell'Università e della Ricerca. NB thanks MIUR for partial financial support of her research grant. The authors would like to acknowledge Chiara Tassone (Erasmus Placement).

References

Bansil R, Turner BS (2006) Mucin structure, aggregation, physiological functions and biomedical applications. Curr Opin Colloid Interface Sci 11:164–170. doi: 10.1016/j.cocis.2005.11.001

Belgorodsky B, Drug E, Fadeev L, et al (2010) Mucin complexes of nanomaterials: First biochemical encounter. Small 6:262–269. doi: 10.1002/smll.200900637

Biale C, Mussi V, Valbusa U, et al (2009) Carbon nanotubes for targeted drug delivery. 2009 9th Ieee Conf Nanotechnol 644–646.

Bomboi F, Bonincontro a., La Mesa C, Tardani F (2011) Interactions between single-walled carbon nanotubes and lysozyme. J Colloid Interface Sci 355:342–347. doi: 10.1016/j.jcis.2010.12.026

Carlstedt I, Sheehan J, Corfield A, Gallagher J (1985) Mucous glycoproteins: a gel of a problem. Essays Biochem 20:40–76.

Chen EY, Daley D, Wang Y-C, et al (2012) Functionalized carboxyl nanoparticles enhance mucus dispersion and hydration. Sci Rep. doi: 10.1038/srep00211

Chen EYT, Wang YC, Chen CS, Chin WC (2010) Functionalized positive nanoparticles reduce mucin swelling and dispersion. PLoS One. doi: 10.1371/journal.pone.0015434

Doerner KC, White BA (1990) Detection of glycoproteins separated by nondenaturing polyacrylamide gel electrophoresis using the periodic acid-Schiff stain. Anal Biochem 187:147–150.

Hattrup CL, Gendler SJ (2008) Structure and function of the cell surface (tethered) mucins. Annu Rev Physiol 70:431–457. doi: 10.1146/annurev.physiol.70.113006.100659

He H, Pham-Huy LA, Dramou P, et al (2013) Carbon nanotubes: Applications in pharmacy and medicine. Biomed Res Int 2013:ID 578290. doi: 10.1155/2013/578290

Lieleg O, Vladescu I, Ribbeck K (2010) Characterization of particle translocation through mucin hydrogels. Biophys J 98:1782–1789. doi: 10.1016/j.bpj.2010.01.012

Liu P (2013) Modification strategies for carbon nanotubes as a drug delivery system. Ind Eng Chem Res 52:13517–13527. doi: 10.1021/ie402360f

Liu Z, Tabakman S, Welsher K, Dai H (2009) Carbon nanotubes in biology and medicine: In vitro and in vivo detection, imaging and drug delivery. Nano Res 2:85–120. doi: 10.1007/s12274-009-9009-8

Loomis RE, Prakobphol A, Levine MJ, et al (1987) Biochemical and biophysical comparison of two mucins from human submandibular-sublingual saliva. Arch Biochem Biophys 258:452–464.

MacAdam A (1993) The effect of gastro-intestinal mucus on drug absorption. Adv Drug Deliv Rev 11:201–220.

MacArthur MW, Thornton JM (1991) Influence of proline residues on protein conformation. J Mol Biol 218:397–412.

Marriott C, Gregory NP (1990) Mucus Physiology and Pathology. In: Lenaerts V, Gurny R (eds) Bioadhesive Drug Delivery Systems. CRC Press, pp 1–24

Mussi V, Biale C, Visentin S, et al (2010) Raman analysis and mapping for the determination of COOH groups on oxidized single walled carbon nanotubes. Carbon 48:3391–3398.

Ronish EW, Krimm S (1974) The calculated circular dichroism of polyproline II in the polarizability approximation. Biopolymers 13:1635–1651.

Saifuddin N, Raziah AZ, Junizah AR (2013) Carbon Nanotubes: A Review on Structure and Their Interaction with Proteins. J Chem 2013:1–18. doi: 10.1155/2013/676815

Scawen M, Allen A (1977) The action of proteolytic enzymes on the glycoprotein from pig gastric mucus. Biochem J

163:363–368.

Sigurdsson HH, Kirch J, Lehr CM (2013) Mucus as a barrier to lipophilic drugs. Int J Pharm 453:56–64. doi: 10.1016/j.ijpharm.2013.05.040

Snary D, Allen A, Pain RH (1970) Structural studies on gastric mucoproteins: Lowering of molecular weight after reduction with 2-mercaptoethanol. Biochem Biophys Res Commun 40:844–851.

Visentin S, Barbero N, Musso S, et al (2010) A sensitive and practical fluorimetric test for CNT acidic site determination. Chem Commun 46:1443–1445.

Viterbo D, Croce G, Frache A, et al (2004) Structural Characterization of Siliceous Spicules from Marine Sponges. 86:526–534. doi: 10.1016/S0006-3495(04)74131-4

Wang R, Mikoryak C, Chen E, et al (2009) Gel electrophoresis method to measure the concentration of single-walled carbon nanotubes extracted from biological tissue. Anal Chem 81:2944–2952. doi: 10.1021/ac802485n

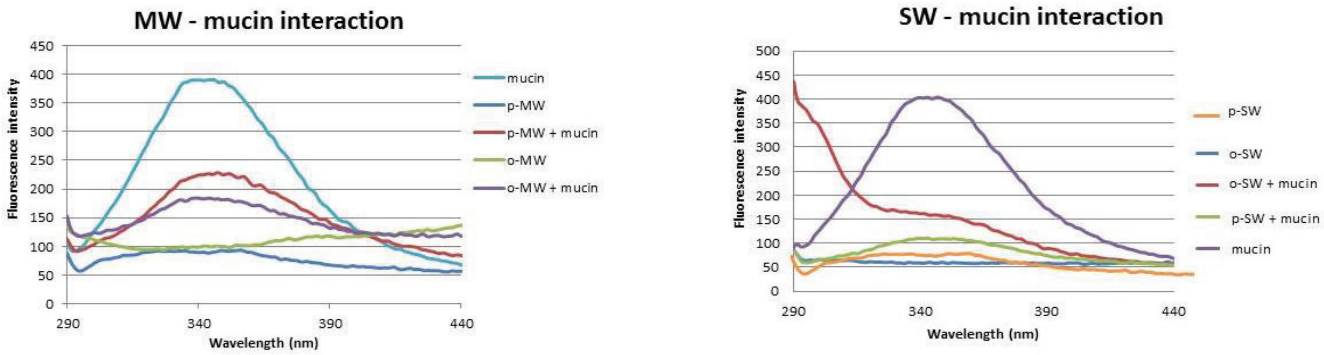

Figure 1. Fluorescence spectra of mucin-CNTs complexes for pristine and oxidized MW (left) and SW (right): comparison with mucin, pristine CNTs and oxidized CNTs alone.

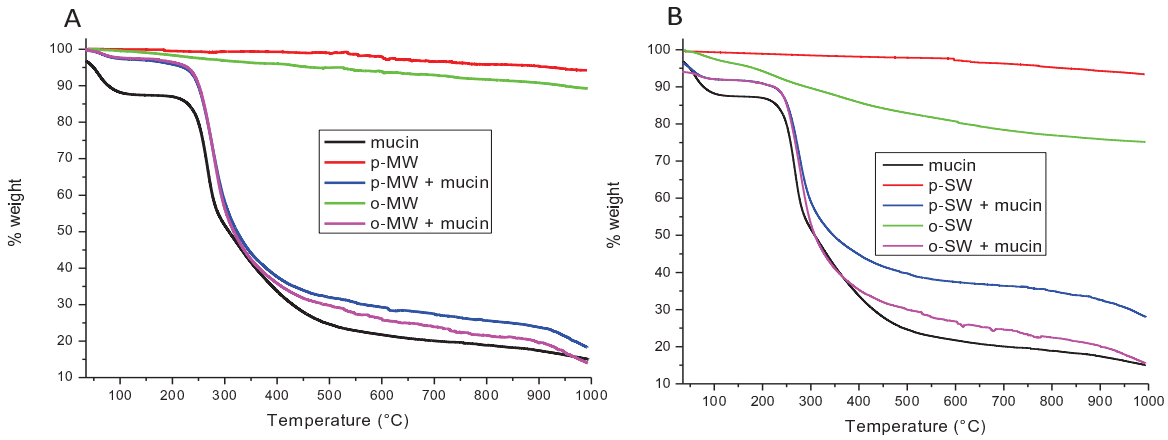

Figure 2. Thermogravimetric analysis in nitrogen flow of: A) mucin (black), p-MW (red), p-MW/mucin (blue), o-MW (green), o-MW/mucin (pink); B) mucin (black), p-SW (red), p-SW/mucin (blue), o-SW (green), o-SW/mucin (pink)

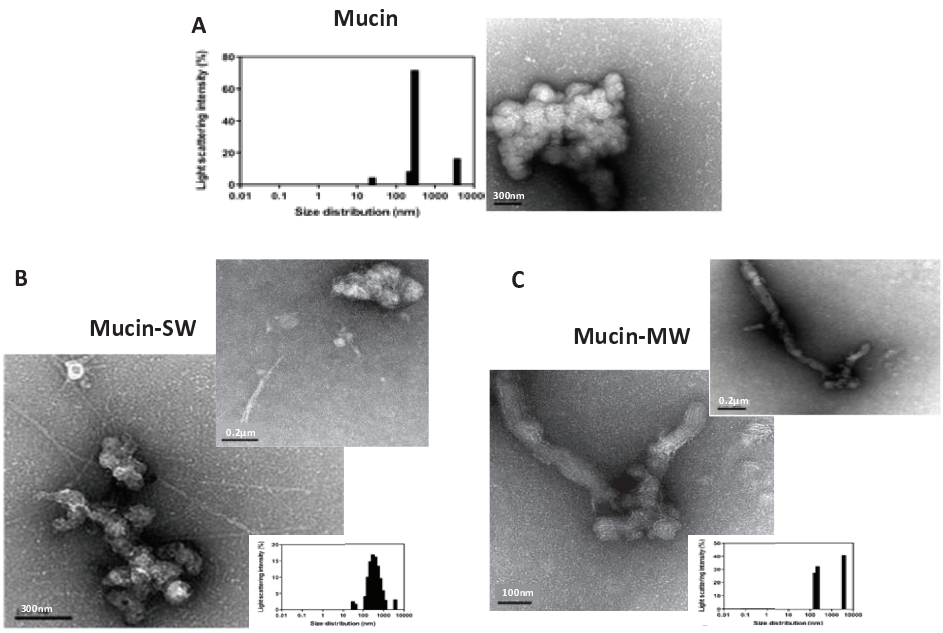

Figure 3. DLS analysis and TEM of A) mucin alone, B) mucin-SW complex, C) mucin-MW complex.

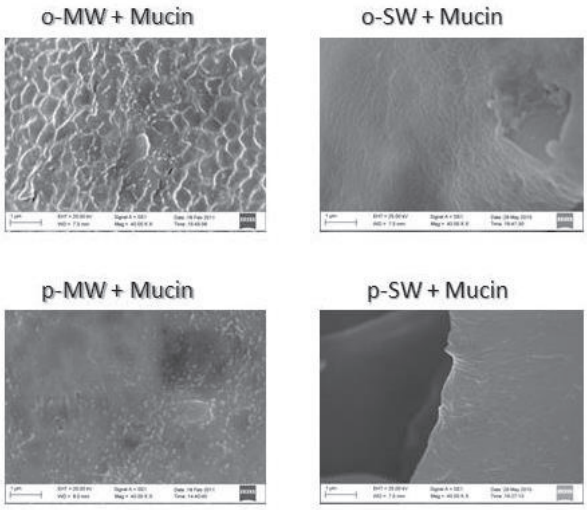

Figure 4. SEM images of MW- and SW-mucin complexes (both pristine and oxidized samples).

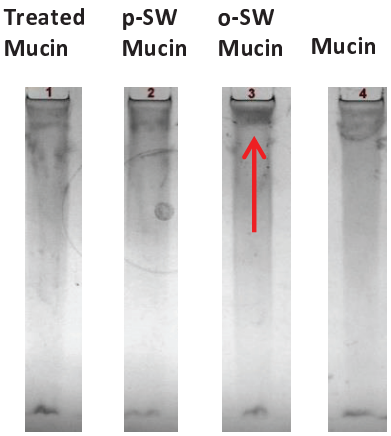

Figure 5. ND-PAGE electrophoresis of 1) mucin (control treated as samples 2 and 3 without the addition of CNTs), 2) mucin/p-SW CNT complex, 3) mucin/o-SW CNT complex, 4) mucin.

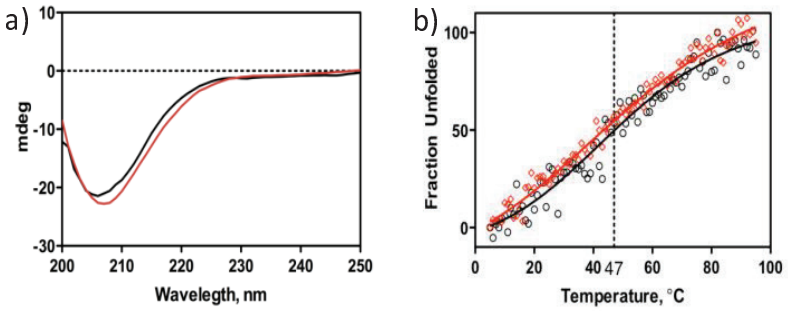

Figure 6. a) Circular dichroism spectra of free mucin in PBS (black) and mucin/o-SW complex (red). b) Thermal unfolding of mucin (black) and mucin/o-SW (red). Solid line represents the best non-linear least-square fitting according to a two state unfolding process.

Supplementary material (audio/video files etc)

Graphical Abstract